Available online at www.sciencedirect.com
ScienceDirect
Thin Solid Films 516 (2008) 7209–7213
thin solid films
www.elsevier.com/locate/tsf

Study of trap states in polyfluorene based devices by using TSC technique

C. Renaud [a], C.H. Huang [b], C.W. Lee [a,b], P. Le Rendu [a], T.P. Nguyen [a,*]

[a] Laboratoire de Physique des Matériaux et Nanostructues, Institut des Matériaux Jean Rouxel, 2 rue de la Houssinière, BP32229, 44322 Nantes, France
[b] Department of Applied Chemistry, National Chiao Tung University, Hsinchu 30010, Taiwan ROC

Available online 14 December 2007

Abstract

The trap states in poly(9,9-dihexylfluorene-co-*N*,*N*-di(9,9-dihexyl-2-fluorenyl)-*N*-phenylamine) (PF-N-Ph) based light emitting diodes have been investigated by using the thermally stimulated current (TSC) technique in the temperature range of 90–320 K. The studied structure consisted of indium-tin-oxide/polyethylene-dioxythiophene: polystyrene-sulfonate/PF-N-Ph/Al. Four traps centers denoted as A, B, C, and D trap types have been identified with densities in the range of 10^{16}–10^{17} cm^{-3}. Study of the dependence of TSC characteristics on the device polarity suggested that the A, C and D type traps are electron traps while the B type traps are hole traps. They can be described by Gaussian distributions centered on mean trap levels.
© 2008 Elsevier B.V. All rights reserved.

Keywords: Traps; Polyfluorene derivative; Thermally stimulated currents

1. Introduction

The transport processes in polymer-based devices such as organic light emitting diodes (OLEDs) have been widely investigated in order to optimize their performance. Recently, several investigations have succeeded in synthesizing of new polyfluorene (PF) family that shows a stable blue electroluminescence, which make them interesting candidates for display applications [1,2]. However, conjugated polymers are well known to contain defect sites in their backbone resulting from their amorphous structure or/and impurities. These defects affect strongly the charge transport properties of polymer-based devices [3–5]. Trapped charge carriers no longer take part in the transport and their charge will influence also the electric field distribution and hence the transport process [6,7]. The determination of energetic distribution of trap states is therefore of key importance for controlling the material electrical properties in order to understand and to optimize charge transport in devices. Several experiments are usually used to investigate the trap states in organic based devices: impedance spectroscopy [8], current–voltage (*I*–*V*) characteristics [9,10], deep level transient spectroscopy (DLTS) [11], and thermally stimulated current (TSC) [12,13]. Energetic trap distributions are estimated by applying space charge limited current (SCLC) models to temperature dependent *I*–*V* characteristics [10]; exponential and/or Gaussian trap distributions have been used to describe mapping of traps in organic based devices [10,13,14]. In the present study, we have used a refined method of the TSC technique, which is the fractional thermally stimulated current (F-TSC) for investigations of traps in PF-N-Ph based devices. It has been proved that this method is suitable for determining the trap state distribution in organic devices [15,16].

2. Experimental

Poly(9,9-dihexylfluorene-co-*N*,*N*-di(9,9-dihexyl-2-fluorenyl)-*N*-phenylamine) (PF-N-Ph), whose chemical structure is shown in the inset of Fig. 1, was synthesized by a method previously reported [16,17], and was dissolved in toluene with a concentration of 6 mg/mL. Indium tin oxide (ITO) coated glass substrates were cleaned in successive ultrasonic baths of distilled water, ethanol and acetone. After drying in nitrogen atmosphere, the substrates were treated by UV ozone before use. A thin layer (40–50 nm) of polyethylene dioxythiophene:

* Corresponding author. Tel.: +33 2 40373976; fax: +33 2 40373991.
E-mail address: nguyen@cnrs-imn.fr (T.P. Nguyen).

0040-6090/$ - see front matter © 2008 Elsevier B.V. All rights reserved.
doi:10.1016/j.tsf.2007.12.063

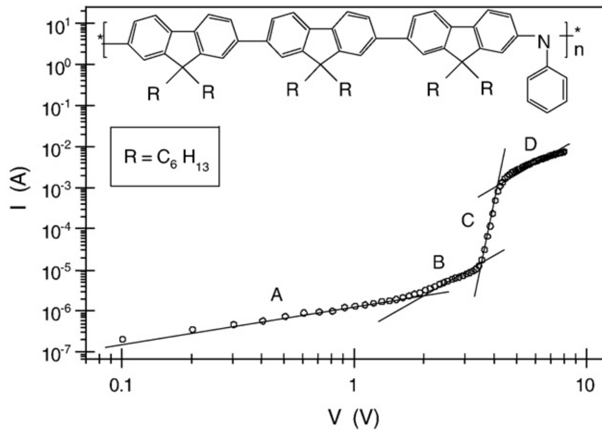

Fig. 1. *I–V* characteristics of ITO/PEDOT/PF-N-Ph/Al structure using double logarithmic scale. Inset is chemical structure of the poly(9,9-dihexylfluorene-co-*N*,*N*-di(9,9-dihexyl-2-fluorenyl)-*N*-phenylamine) (PF-N-Ph).

polystyrene sulfonate (PEDOT:PSS) was deposited on the ITO substrate, which was then annealed at 150 °C for 1 h under vacuum. The polymer film of thickness about 70–80 nm was spin-coated onto the PEDOT-PSS film, and the fabrication of the device was achieved with deposition of an aluminum cathode under high vacuum conditions ($<10^{-6}$ mbar). The devices were encapsulated with a glass coverlid using an epoxy resin. The structure of the studied devices is ITO/PEDOT:PSS/PF-N-Ph/Al.

TSC experiments were carried using a cryostat whose temperature was controlled by an Oxford ITC 503 U. A Keithley 230 programmable voltage source coupled with a Keithley 617 electrometer was used for monitoring the TSC spectra. Several TSC techniques are available for determination of traps in semiconductors [18,19]. The measurement procedure used in this study was as follows. At a high temperature T_H, a voltage V_H was applied to the device during a charging time t_C of 5 min. The sample was then cooled to low temperature T_L with the applied voltage V_H and then was short-circuited. After being allowed to reach an equilibrium state, the sample is heated at a constant heating rate $\beta = dT/dt$ and the current is recorded as function of the temperature, giving the TSC spectrum. By modifying the charging voltage V_H, one can expect to observe the charge released from the electron or the hole traps depending on the polarity of the sample. The analysis of the TSC spectrum is based on theoretical treatments. By integrating the released current over time, the amount of trapped charges ΔQ is obtained and the average trap density N_T can be evaluated by the following relation:

$$N_T = \frac{\Delta Q}{eAd} \tag{1}$$

where e is the electronic charge, A is the surface, and d is thickness of the sample.

Assuming that re-trapping of released charge carriers is negligible and that the probability for a carrier to escape from a trap obeys to Boltzmann statistics, Cowell and Woods [20] derived the following relation for TSC:

$$I(T) = N_{t0}.s.\exp\left(-\frac{E_t}{kT}\right).\exp\left(-\frac{s}{\beta}\right)\int_{T_0}^{T}\exp\left(-\frac{E_t}{kT'}\right)dT' \tag{2}$$

where N_{t0} and T_0 are the initial concentration and temperature of trapped charge carrier respectively, k is Boltzmann constant, s is the frequency factor, T is the absolute temperature and E_t is the activation energy, which was determined by initial rise method [20].

To get information on trap distribution, fractional TSC experiments were carried out [21]. The technique consists of performing a series of subsequent initial rise measurements where only a small fraction of trap is emptied. The remaining trap population is constant during each heating cycle. By choosing the convenient end temperature for each cycle, successive emission of carriers occurs with repetition of cooling-heating process, and it is then possible to determine the activation energy and the trap density distribution.

3. Results and discussion

3.1. Current–voltage and luminance characteristics

Fig. 1 shows the current–voltage characteristics of ITO/PEDOT:PSS/PF-N-Ph/Al at $T = 300$ K and plotted on a double logarithmic scale. The forward current was obtained with a positive bias applied to the ITO substrate. We have limited the applied voltage at +8 V in order to limit damage risks of the active layer. The diode shows a turn-on voltage $V_{TO} \sim 4$ V. The *I–V* characteristics can be described by the space-charge-limited current (SCLC) model. Four distinct regions labeled A, B, C and D, appear clearly in Fig. 2, with slope values of ~1.2, ~2.1, ~23.8, and ~2.1 respectively. A similar behaviour has been also observed at room temperature in polyfluorene based diodes

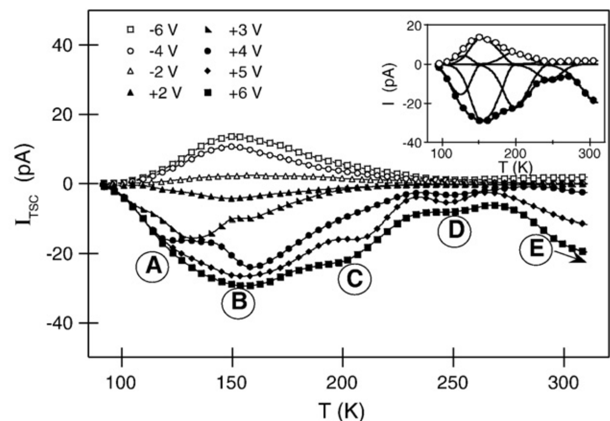

Fig. 2. TSC spectra recorded in a ITO/PEDOT/PF-N-Ph/Al diode using the following parameters: $T_H = 300$ K, $\beta = 0.1$ K/s, with different charging voltages: $V_C = -6$ V, −4 V, −2 V, +2 V, +3 V, +4 V, +5 V, +6 V. Inset is the decomposition of the TSC spectrum obtained with the following parameters: $T_H = 300$ K, $\beta = 0.1$ K/s, $V_C = +6$ V (●) and $V_C = -6$ V (○) by using the computed curves from the Eq. (5) with the activation energies determined from the Arrhenius plots.

Table 1
Trap parameters obtained from decomposition of TSC spectrum and fractional TSC experiments with V_H=6 V

Peak	T (K)	E_a (eV)	N_T (cm^{-3})	σ (eV)	N_M (cm^{-3})
A	124	0.13	2.4×10^{16}	0.035	1.6×10^{14}
B	153	0.22	6.1×10^{16}	0.051	1.4×10^{15}
C	198	0.33	4.4×10^{16}	0.035	1.4×10^{14}
D	247	0.45	1.5×10^{16}	0.022	9.4×10^{13}
E	>320	0.59	$>2.7\times10^{16}$	X	X

[22]. The current flow is nearly ohmic at low forward applied voltages and close to trap-free space charge limited at high voltages (>4 V). According to the SCLC analysis, region B corresponds to the shallow trapping regime and region C to the filling of deeper traps [10,23]. An estimation of the trap density N_T from the transition voltage V_{TFL} (trap free limited voltage) between trap filling and trap free regions can be obtained by the following expression [24]:

$$V_{TFL} = \frac{eN_T L^2}{2\varepsilon} \tag{3}$$

where L is the film thickness and ε is the permittivity of the semiconductor. As $V_{TFL}\sim4.3$ V and $\varepsilon=\varepsilon_r\varepsilon_0\sim2.4\times10^{-11}$F m^{-1}, assuming a single trap level, we obtained $N_T\sim2\times10^{17}$ cm^{-3}. It will be shown later on that traps in the polymer are distributed in reality, but a simple calculation allowed us to estimate the trap density from I–V characteristic.

An alternative interpretation of the I–V characteristic can also consider two types of traps for regions B and D, region C being the transition region between them. Each region (B or D) could correspond to a trap limited conduction regime, whose current is given by [24,25]:

$$I = \frac{9}{8}\varepsilon\mu\theta\frac{V^2}{L^3}S \tag{4}$$

where S is the active surface of the diode, θ is the trapping fraction and μ is the carrier mobility. Both trapping regimes would lead to the quadratic dependence of J on V as observed, but with different trap parameters.

The electroluminescence and photoluminescence characteristics of device display a peak at 442 nm with a blue light and a shoulder at 462 nm (not shown here).

3.2. TSC measurements

Fig. 2 shows the TSC spectra obtained with different charging voltages: V_C=−6 V, −4 V, −2 V, +2 V, +3 V, +4 V, +5 V, +6 V. The TSC spectra intensity increased with the applied voltage as observed in TSC measurements of OLEDs [26] indicating that the trap filling depends on the bias condition. In the reverse direction, a large width peak appears distributed in the temperature range [100–230 K]. In the forward direction, in addition to a broader peak defined between 100 K and 230 K, two shoulders appear clearly at ~124 K and ~200 K respectively for applied voltages higher than 2 V indicating that additional trapped charges are released. The TSC peaks are denoted as A, B, C, and D. Peaks A, C and D depend strongly on the applied voltage, and appear when $V_H>V_{TO}$ suggesting that they are minority-like traps. Furthermore, at high temperature (>300 K), we note that the onset of an additional peak labeled E, which is visible in both directions.

Because of the overlapping of peaks A, B, C and D, it is necessary to separate those peaks by the peak decomposition technique. By assuming first order kinetics process [18], the temperature dependence equation of the TSC current for traps that are distributed in energy between two levels E_1 and E_2 can be written from Eq. (2):

$$I(T) = \int_{E_1}^{E_2} N(E).\exp\left(-\frac{E_t}{kT}\right).\exp\left[-\frac{s}{\beta}\int_{T_0}^{T}\exp\left(-\frac{E_t}{kT'}\right)dT'\right]dE \tag{5}$$

where $N(E)$ is the energetic distribution of the charge density.

The inset of Fig. 2 shows the decomposition of TSC spectra obtained with V_H=+6 V and V_H=−6 V using the fitting curve to evaluate the activation energy and the trap density. It is noted that the intensity of the peaks are lower in reverse direction than in forward direction. The decomposition of TSC spectrum with V_H=−6 V shows that the intensity of peaks A, C and D are smaller than that of peak B suggesting that the latter is related to the injection of majority carrier. While at V_H=+6 V, peaks A, C and D have stronger intensity indicating that they are related to minority carriers. As peak E is not entirely visible, we could not identify clearly its type (electron or hole traps). The trap parameters determined from the decomposition analysis are summarized in Table 1. Note that the trap density of the level E represents the inferior limits because the corresponding TSC peak is not entirely visible.

Next, we have investigated the energetic trap distribution in diodes by fractional TSC measurements whose technique was previously described [15,27]. Fig. 3 shows the set of fractional TSC spectra recorded in the temperature range of [90–320 K] with V_H=+6 V by using temperature intervals of ΔT=15 K. The activation energy E_{Ti} of each component was determined by the initial rise technique and the partial trap density N_{Ti} was determined from Eq. (1). To determine the distribution of traps for each peak, we used the evaluation technique of TSC curves

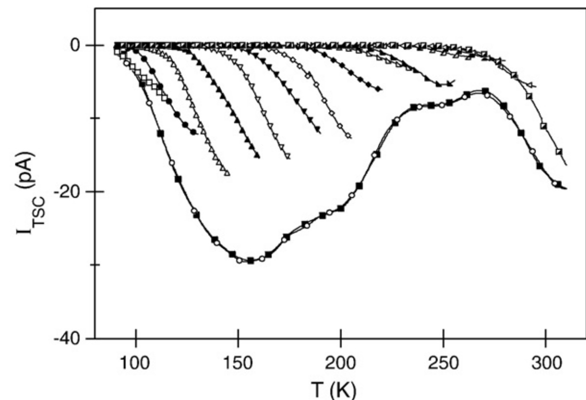

Fig. 3. Fractional TSC spectra in a ITO/PEDOT/PF-N-Ph/Al diode in temperature range 90–320 K with T_H=300 K, V_C=+6 V at different heating cycles.

proposed by Cowell and Woods [20]. Assuming no re-trapping, each fractional spectrum is computed making use of the activation energy E_{Ti} and the trap density N_{Ti} determined from the experimental curve. Trap distribution obtained from data for V_H=+6 V is shown in Fig. 4. Furthermore, for peaks A, B, C and D, the charge density can be described by using Gaussian distribution of traps [18]:

$$N(E) = \frac{N_M}{\sigma\sqrt{2\pi}}.\exp\left(-\frac{(E-E_M)^2}{2\sigma^2}\right) \quad (6)$$

where E_M is the mean value of the trap level, N_M is the density of trapped charge, and σ is the standard deviation representing the width of the distribution.

The distribution corresponding to peak B is centered at E_T=0.22 eV for both directions and is assigned to majority-like traps. Peaks A, C and D, centered at E_T=0.13 eV, 0.33 eV and 0.45 eV, are assigned to carriers released from minority-like trap centers since they strongly increased in intensity when the applied voltage is higher than V_{TO}. Table 1 summarizes the simulation parameters used for describing the distribution obtained with V_H=6 V. Poplavskyy et al. [28] have shown that the interface PEDOT:PSS/polyfluorene is an ohmic contact. In addition, the hole mobility in PF materials is higher than electron mobility suggesting that PF is hole transport material [29]. Type B traps are hole-like acceptor traps and can be originated from PF structure as determined in PF where hole traps with an activation energy of ~0.24 eV [3]. These traps were suggested to be introduced in the polymer backbone as hole transporting moieties at the chain ends.

In addition, electron like traps with activation energy of ~0.6 eV were also identified in PF, and were assigned to on-chain keto defects [3]. These traps would correspond to type E traps in our samples. However, the nature of type E traps is not clearly established because we could observe only the onset of corresponding TSC peak. Formation of keto defects is accompanied by a low energy emission band at 2.2–2.3 eV caused by the photooxydation of polyfluorenes and hence a green emission peak around 550±10 nm is clearly observed in the EL spectrum of OLEDs [4,5]. However, the EL spectrum in our diodes does not show clearly this green emission and does not allow us to conclude on the nature of the type E traps. Concerning the type A, C and D traps, they are electron-like traps. The PF-N-Ph has an energetic band gap of 2.81 eV [11,30]. The PL and EL spectra display the emission peaks at 2.80 eV and 2.68 eV, which are assigned to $\pi * -\pi$ transition and the delocalized π-electron system of PF main chain. We note that the type A traps introduce a level localized at 2.68 eV within the band gap of PF-N-Ph corresponding to emission peak at 462 nm. This observation suggests that the type A electron traps would probably act like recombination traps and hence would be likely originated from the PF chain. The origin of the type C and D electron traps could not be clearly established. Nevertheless, several studies [27,31–33] have been reported that the PEDOT:PSS would probably introduce interfacial electron traps that result in the more efficient hole injection in PF. In addition, Kadashchuk et al. [3] have studied PF materials based diodes without PEDOT:PSS diodes by TSC experiment, and did not observe electron-like traps localized at 0.33 eV and 0.45 eV from the LUMO band. Comparing their results with ours, the additional trap levels can be attributed to the presence of defect states issuing from the interfacial region between PEDOT:PSS injection layer and the PF emission layer. Such defects have been already observed in diodes using poly(9,9-dioctylfluorene-*alt*-benzothiadiazole) (F8BT) as an active layer [33].

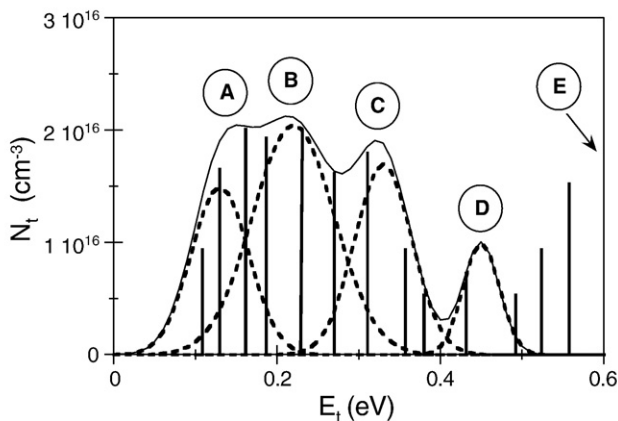

Fig. 4. Distribution of traps in a ITO/PEDOT/PF-N-Ph/Al diode obtained from fractional TSC measurements with V_C=+6 V. Simulation parameters: σ_A=0.035 eV, E_{MA}=0.13 eV, $N_{MA}=1.3\times10^{15}$ cm^{-3} (type A). σ_B=0.051 eV, E_{MB}=0.22 eV, $N_{MB}=2.6\times10^{15}$ cm^{-3} (type B). σ_C=0.035 eV, E_{MC}=0.33 eV, $N_{MC}=1.5\times10^{15}$ cm^{-3} (type C). σ_D=0.022 eV, E_{MD}=0.45 eV, $N_{MD}=5.5\times10^{14}$ cm^{-3} (type D).

4. Conclusion

In this study, we have investigated the defect states in poly (9,9-dihexylfluorene-co-*N*,*N*-di(9,9-dihexyl-2-fluorenyl)-*N*-phenylamine) (PF-N-Ph) based diodes by using the TSC technique. Analyses of the TSC spectra as function of the polarity of the device have revealed the presence of hole-like donor traps located at E_{TB}~0.22 eV from the HOMO band and three trap levels identified like electron traps situated at E_{TA}~0.13 eV, E_{TC}~0.22 eV and E_{TD}~0.45 eV from the LUMO. Gaussian distributions could be applied to describe the trap density of all the levels. One type of traps is assigned to electron traps, which act as emissive recombination centers. They are likely defects in the polymer backbone. The hole traps (type B) can be attributed to moieties at chain ends of the polymer, as suggested previous investigations on PF based devices. Two other electron trap levels are tentatively associated to the interfacial region formed between PEDOT and the polymer but further investigations are needed to clearly establish their origin. Finally, the TSC technique is efficient in studying defects in organic semiconductors and is useful for optimizing the material processing parameters.

References

[1] A.J. Cadby, P.A. Lane, H. Mellor, S.J. Martin, M. Grell, C. Giebeler, D.D.C. Bradley, M. Wohlgenannt, C. An, Z.V. Vardeny, Phys. Rev., B 62 (2000) 15604.

[2] U. Scherf, E.J.W. List, Adv. Mater. 14 (2002) 477.
[3] A. Kadashchuk, R. Schmechel, H. von Seggern, U. Scherf, A. Vakhnin, J. Appl. Phys. 98 (2005) 024101.
[4] E.J.W. List, R. Guentner, P.S. de Freitas, U. Scherf, Adv. Mater. 14 (2002) 374.
[5] S. Gamerith, C. Gadermaier, U. Scherf, E.J.W. List, Phys. Status Solidi 201 (2004) 1132.
[6] P.H. Nguyen, S. Scheinert, S. Berleb, W. Brütting, G. Paasch, Org. Electron. 2 (2001) 105.
[7] O. Gaudin, R.B. Jackman, T.P. Nguyen, P. Le Rendu, J. Appl. Phys. 90 (2001) 4196.
[8] A.J. Campbell, D.D.C. Bradley, D.G. Lidzey, J. Appl. Phys. 82 (1997) 6326.
[9] P.E. Burrows, Z. Shen, V. Bulovic, D.M. McCarty, S.R. Forrest, J.A. Cronin, M.E. Thompson, J. Appl. Phys. 79 (1996) 7991.
[10] S. Berleb, A. Mückl, W. Brütting, M. Schwoerer, Synth. Met. 111–112 (2000) 341.
[11] H.L. Gomes, P. Stallinga, H. Rost, A.B. Holmes, M.G. Harrison, R.H. Friend, Appl. Phys. Lett. 74 (1999) 1144.
[12] S. Karg, J. Steiger, H. Von Seggern, Synth. Met. 111–112 (2000) 277.
[13] J. Steiger, R. Schmechel, H. Von Seggern, Synth. Met. 129 (2002) 1.
[14] W. Brütting, S. Berleb, A.G. Mückl, Org. Electron. 2 (2001) 1.
[15] R. Schmechel, H. Von Seggern, Phys. Status Solidi 201 (2004) 1215.
[16] H. Gobrecht, D. Hofmann, J. Phys. Chem. Solids 27 (1966) 509.
[17] G. Kläerner, R.D. Miller, Macromolecules 31 (1998) 2007.
[18] R. Chen, Y. Kirsh, Pergamon, Analysis of Thermally Stimulated Processes, Pergamon Press Ltd, Oxford, 1981 (Ch. 1).
[19] J. Vauderschueren, J. Gasiot, in: P. Braülich (Ed.), Thermally Stimulated Relaxation in Solids, Springer Verlag, 1979, (Ch. 4).
[20] T.A.T. Cowell, J. Woods, Br. J. Appl. Phys. 18 (1967) 1045.
[21] H. Gobrecht, D. Hofmann, J. Phys. Chem. Solids 27 (1966) 509.
[22] M. Arif, M. Yun, S. Gangopadhyay, K. Ghosh, L. Fadiga, F. Galbrecht, U. Scherf, S. Guha, Phys. Rev., B 75 (2007) 195202.
[23] A.J. Campbell, D.D.C. Bradley, D.G. Lidzey, Opt. Mater. 9 (1998) 114.
[24] K.C. Kao, Dielectric Phenomena in Solids, Pergamon Press, Oxford, 1981.
[25] F. Schauer, Sol. Energy Mater. Sol. Cells 87 (2005) 235.
[26] A.G. Werner, J. Blochwitz, M. Pfeiffer, K. Leo, J. Appl. Phys. 90 (2001) 123.
[27] N. Von Malm, J. Steiger, H. Heil, R. Schmechel, H. Von Seggern, J. Appl. Phys. 92 (2002) 7564.
[28] D. Poplavskyy, J. Nelson, D.D.C. Bradley, Appl. Phys. Lett. 83 (2003) 707.
[29] M. Redecker, D.D.C. Bradley, M. Inbasekaran, E.P. Woo, Appl. Phys. Lett. 73 (1998) 1565.
[30] F. Uckert, Y.H. Tak, K. Müllen, H. Bässler, Adv. Mater. 12 (2000) 905.
[31] K. Murata, S. Cinà, N.C. Greenham, Appl. Phys. Lett. 79 (2001) 1193.
[32] P.A. Lane, J.C. deMello, R.B. Fletcher, M. Bernius, Appl. Phys. Lett. 83 (2003) 3611.
[33] P.J. Brewer, P.A. Lane, J. Huang, A.J. deMello, D.D.C. Bradley, J.C. deMello, Phys. Rev., B 71 (2005) 205209.